

## Phase and envelope characteristics of ultrashort pulses reflected from a two-dimensional silicon photonic crystal

H. W. Tan and H. M. van Driel

*Department of Physics and Institute for Optical Sciences, University of Toronto, 60 St. George Street, Toronto, Ontario, Canada M5S1A7*

S. L. Schweizer and R. B. Wehrspohn

*Nanophotonics Materials Group, Department of Physics, University of Paderborn, 33095 Paderborn, Germany*

(Received 16 September 2005; revised manuscript received 26 April 2006; published 24 July 2006)

We experimentally demonstrate how coherent Bragg, and incoherent, multiple scattering influence the phase characteristics and the temporal shape of 35 nm bandwidth, 200 fs optical pulses specularly reflected in the plane of periodicity from a two-dimensional (2D) silicon photonic crystal with 560 nm diameter air holes and a 700 nm pitch. The pulse center wavelength was chosen to lie (i) inside a 1320–1600 nm photonic band gap; (ii) on the short wavelength gap edge, or (iii) outside the photonic band gap. The shape of Bragg reflected pulses [case (i)] differs insignificantly from the incident pulse as expected, whereas for pulses whose center wavelength is outside the band gap [case (iii)], multiple diffuse scattering distorts the pulse shape, and the pulse width is broadened by as much as 48%, depending on the illumination site. For pulses centered on the band edge [case (ii)], the group delay is reduced by as much as  $\sim 45$  fs in certain spectral regions compared to Bragg reflected light. Bragg scattering dominates other scattering processes and the reflected pulse shape is mainly governed by the asymmetric reflectivity spectrum and the input pulse characteristics such as bandwidth and chirp. The difference between the mean free path of Bragg scattered photons and surface scattered photons is estimated to be  $6 \mu\text{m}$ .

DOI: [10.1103/PhysRevB.74.035116](https://doi.org/10.1103/PhysRevB.74.035116)

PACS number(s): 39.30.+w, 42.70.Qs, 78.47.+p, 82.53.Mj

### I. INTRODUCTION

The unusual dispersive properties of photonic crystals (PhCs) have been the subject of considerable fundamental and applied research.<sup>1–11</sup> Optical properties such as reflectivity or transmissivity are often measured using monochromatic or incoherent, broadband light sources. In most cases the data provide only intensity but no phase information. The propagation of narrow bandwidth optical pulses in PhCs (Refs. 3–6) has also been studied with interferometric techniques and revealed group velocity dispersion characteristics that are not easily obtained using monochromatic beams. In the measurements of Imhof *et al.*<sup>5</sup> and Tanaka *et al.*<sup>6</sup> pulse reshaping due to group velocity dispersion in the vicinity of a stop-gap was also hinted at although no direct measurements were made.

While the properties of ideal, or assumed ideal, PhCs, including those with well-defined waveguides or microresonators, can, in principle, be calculated using Maxwell's equations,<sup>1</sup> actual fabricated PhCs are never ideal<sup>7</sup> and experiments are necessary to obtain the complete properties. Besides coherent Bloch wave propagation and Bragg scattering, incoherent multiple and diffuse scattering influence the optical properties via the complex dispersion characteristics or structural imperfections. Here, using frequency resolved optical grating (FROG) techniques we show how the envelope and phase characteristics of broad bandwidth femtosecond optical pulses are modified upon reflection from a two-dimensional (2D) silicon PhC prepared by electrochemical etching techniques. Using finite difference time-domain (FDTD) analysis we corroborate some of the experimental findings related to the underlying ideal PhC.

In earlier studies that employed optical pulses with small bandwidths, properties such as group velocity dispersion were obtained by varying the pulse center wavelength.<sup>5</sup> In our case, the pulse bandwidth ( $\sim 35$  nm) is large compared to the nonzero width of the actual Bragg gap edge and one obtains direct evidence of pulse reshaping and distortion as well as aspects of the interplay between coherent and incoherent scattering related to crystal imperfections. Because of the short interaction length of light reflected from a medium, short pulses are ideally suited to provide information on dispersion and phase properties. Overall we find the reflected pulse characteristics depend on the relative wavelengths of the pulse and photonic band gap edge. The experimental results show the influence of incoherent and coherent scattering mechanisms, aspects that cannot be deduced from band structure calculations of ideal PhCs. From the spectral phase of the reflected pulses, we infer the corresponding group delay and thus deduce the photon mean free path for the reflected light.

When the center wavelength falls within the photonic gap, Bragg reflectivity is dominant, and from the essentially unaltered reflected pulse envelope, we infer that the sample is essentially periodic with some disorder in the near-surface region limiting the maximum reflectivity. However, when the center wavelength of the pulse falls at or on the short wavelength side of the band edge, the experimental results reveal several interesting features relative to what one would expect from an ideal PhC.

(i) When the center wavelength is the band edge, the asymmetry of the reflectivity spectrum leads to significant pulse reshaping and a spectral dependence of the group delay. At the band edge wavelength there is a negligible in-

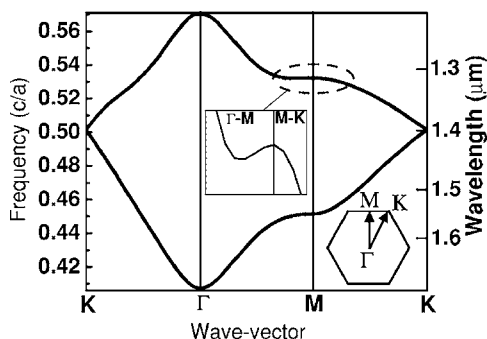


FIG. 1. Dispersion curves of lowest lying modes for the PhC near the wavelengths of experimental interest. The inset is a magnified portion of the band structure close to the band edge.

crease in the group delay relative to that experienced by wavelengths away from the edge, contrary to what one may expect from band structure calculations.<sup>5</sup> This may be related to the small penetration depth of the reflected pulses in the PhC and/or incoherent scattering processes. Indeed, there is a *decrease* in the group delay for wavelength  $\sim 10$  to  $20$  nm below the band edge. We attribute these dips in the group delay to possible mode interference and light refraction effects.

(ii) When the pulse center wavelength and bandwidth lie outside the band gap, significant distortion in the pulse shape is observed and the pulse is broadened by as much as 48%. We suggest that this is related to multiple diffuse scattering<sup>8–10</sup> wherein reflected photons traverse a distribution of path lengths in the PhC. There is also a strong variation in the group delay across the pulse spectrum. From the group delay information, the difference in the mean free paths for Bragg scattered photons and incoherently scattered photons in the near-surface region is estimated to be  $\sim 6$   $\mu\text{m}$ . The photon mean free path is unique to the sample used and is a result of the multiple coherent and incoherent scattering processes. Previously, estimates of this distance could only be obtained by studying the spatial characteristics of backreflected light.<sup>11</sup> We show here that one can also obtain this information by studying the phase and shape characteristics of reflected pulses.

The remainder of this paper is organized as follows. In Sec. II we provide details of the 2D silicon PhC sample and the optical techniques used in the experiments. In Sec. III we discuss the FDTD simulations while Sec. IV provides the experimental results and comparison with the simulations. We end with some conclusions in Sec. V.

## II. EXPERIMENTAL DETAILS

The  $6 \times 7$   $\text{mm}^2$  2D silicon PhC sample used in the experiments has a triangular lattice arrangement of 560 nm diameter and 96  $\mu\text{m}$  deep air holes with a pitch of 700 nm. Figure 1 shows the relevant bands of the PhC accessed in this work. Of particular interest to us is the shorter wavelength edge of a photonic gap (1320–1600 nm) for *E*-polarized (*E*-field directed along pore axis) light propagating along the  $\Gamma$ -*M* direction (normal to a face of the PhC). To study the pulse

reflectivity characteristics of these samples, 200 fs pulses [full width at half maximum (FWHM)] in the wavelength range 1200–1500 nm and with peak power  $< 180$  kW were obtained from an optical parametric amplifier pumped by a 250 kHz repetition rate Ti-sapphire oscillator/regenerative amplifier. To eliminate spurious diffuse scattering from the PhC substrate, the pulses were focused at normal incidence onto the sidewalls of the PhC with a spot diameter of 30  $\mu\text{m}$ .<sup>12</sup> The angular convergence of the incident beam was  $\sim 0.1$  rad. The detection optics were located  $\sim 1$  m from the PhC surface so that most of the collected light is specularly reflected.

For the reflectivity measurements the center wavelength of the 35 nm bandwidth pulses was tuned to  $\lambda_{\text{out}} = 1260$  nm (outside the photonic gap),  $\lambda_{\text{edge}} = 1320$  nm (on the band edge) or  $\lambda_{\text{in}} = 1340$  nm (within the photonic gap). Measurements of the reflectivity, normalized to the incident pulse intensity were taken on several well-separated sites on the sample sidewall so that common features related to the optical characteristics of the sample could be identified and the effects of variations in the PhC termination are minimized. The reflected pulses were analyzed using a FROG technique<sup>13</sup> based on second harmonic generation in a 160  $\mu\text{m}$  thick type I BBO crystal.<sup>14</sup> Although the BBO crystal was oriented to achieve maximum conversion efficiency for the polarization conserved (*s*-polarized) component of specular reflected light, no significant amount of depolarization is observed. This suggests that scattering in the direction normal to the plane of periodicity (i.e., the plane of incidence) is not as important as in-plane scattering for the specular reflected light. As a check for any systematic errors, the retrieved spectra from the FROG experiments were compared with directly measured spectra obtained with a 0.25 m monochromator. Little difference ( $< 5\%$ ) was observed between the retrieved and measured spectra.<sup>15</sup> In order to determine the direction of time in the retrieved FROG traces, the pulses were deliberately chirped by passing them through two SF2 polarizing beam cubes<sup>16</sup> before they were incident on the sample. The 220 fs pulses incident on the samples had a bandwidth of 35 nm (FWHM) and a spectral chirp  $d^2\phi(\omega)/d\omega^2 \sim 1.6$   $\text{fs}^2/\text{mrad}$  where  $\phi(\omega)$  is the spectral phase and  $\omega$  the angular frequency.

Figure 2 shows typical reflectivity spectra in the vicinity of the 1320 nm band edge at different sample sites. Structural imperfections such as irregularities in the sizes and positions of the cylindrical air holes, and surface roughness, contribute to the varying spectral features of the spectra. Note, however, that every spectrum shows a prominent minimum on the short wavelength side of the band edge with a drop that varies from 2% to 8% of the peak reflectivity. The origin of these minima is discussed below.

## III. SIMULATIONS

The spectral and temporal reflectivity characteristics were simulated using FDTD techniques. In the simulations, Gaussian shaped pulses were launched into a 2D PhC with the same characteristics as those used in the experiments but which had 300 lattice rows and a front surface that had a

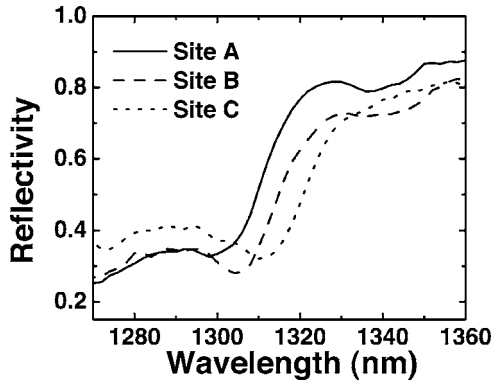


FIG. 2. Experimental reflectivity spectra in the vicinity of the 1320 nm band edge at different sites on the PhC sample. The spectra are normalized by the incident pulse spectrum.

well-defined termination, viz., a series of semicircular cylinders. Pulses reflected from PhCs with other surface terminations were found to produce much less pronounced but similar features depending on how well the external light couples to the PhC sample. The hemispherical surface termination corresponds most closely to the experimental sample characteristics; the 2D samples of the type we use cleave most easily at the thin silicon necks.

The incident optical pulses used in the simulations were positively chirped and have the same bandwidth and pulse width as those used in the experiments. The sample length is chosen so that the transmitted pulse does not reach the end of the sample before the first reflected pulse is detected; this eliminates interference effects between back surface and front surface reflected pulses. Because of the short interaction length of the reflected pulses with the PhC, material dispersion is not expected to significantly influence pulse reshaping. For example, transform-limited 73 fs Gaussian pulses in the 1200–1500 nm range are expected to be broadened by  $<0.3\%$  after traversing 100  $\mu\text{m}$  of bulk silicon (equivalent to 2 passes through 200 PhC rows in the  $\Gamma$ - $M$  direction) for which the group velocity dispersion is  $6 \text{ fs}^2/\mu\text{m}$ . Two photon absorption of the optical pulses can also be neglected since the attenuation depth of our pulses with focused intensities of  $<10 \text{ GW}/\text{cm}^2$  (for a two photon absorption coefficient of  $\sim 1 \text{ cm}/\text{GW}$ ) is  $>500 \mu\text{m}$  which is equivalent to a single pass through 1800 PhC rows in the  $\Gamma$ - $M$  direction. Indeed, variation of the peak power between 55 and 180 kW produces no measurable difference in the experimental results indicating a negligible influence of nonlinear optical effects in general.

#### IV. RESULTS AND ANALYSIS

Figure 3 presents results for the experimentally determined and simulated temporal pulse shapes for  $\lambda_{\text{in}}$ ,  $\lambda_{\text{out}}$ , and  $\lambda_{\text{edge}}$  pulses. For each of the panels within the figure the incident pulse profile as well as the reflectivity from three different sites is indicated. Figures 4(a)–4(c) show the corresponding spectral intensity and phase profiles for the pulses. From the spectral phase of the pulses one can derive the spectral group delay  $\tau_g = d\phi(\omega)/d\omega$ . Figures 4(a') to 4(c')

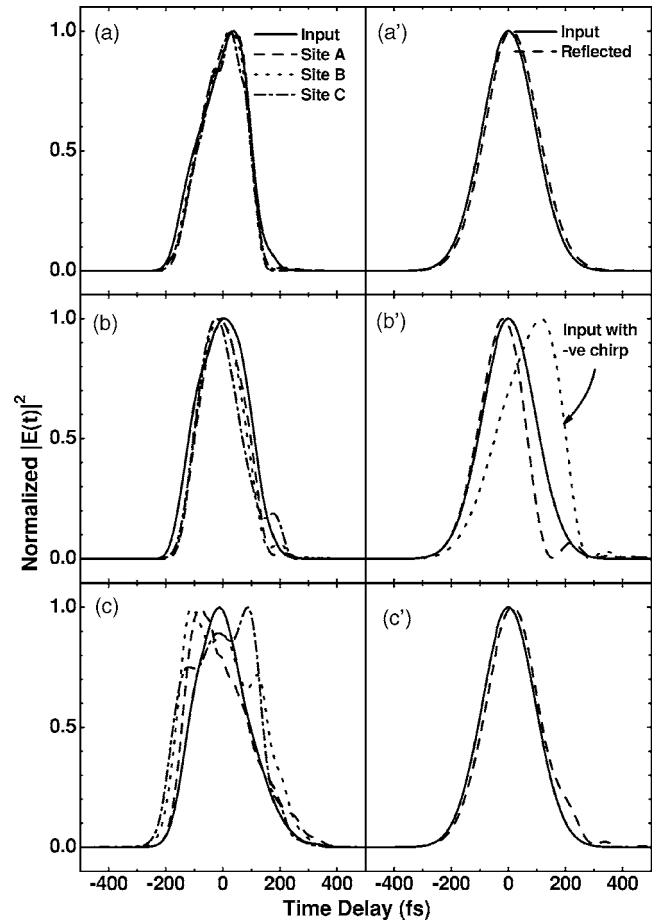


FIG. 3. The input and reflected pulse temporal shapes for  $\lambda_{\text{in}}$ ,  $\lambda_{\text{edge}}$ , and  $\lambda_{\text{out}}$  pulses. Frames (a) to (c) are the experimentally determined profiles for  $\lambda_{\text{in}}$ ,  $\lambda_{\text{edge}}$ , and  $\lambda_{\text{out}}$  pulses respectively while frames (a') to (c') are the corresponding simulated traces.

show the extracted differential group delay which is obtained by subtracting the group delay of the input pulse from that of the reflected pulses; this enables the influence of the PhC to be isolated.

We discuss each of the three wavelength cases in turn.

(i) *Pulse centered within the phonic band gap.* The experimental temporal shapes of the reflected  $\lambda_{\text{in}}$  pulses<sup>17</sup> are shown in Fig. 3(a'). They exhibit little change from the incident pulse, also shown. This is in good agreement with the FDTD simulation results shown in Fig. 3(a'). In this wavelength regime, coherent Bragg diffraction is the dominant contribution to the sample reflectivity and one could infer the order of crystallinity close to the sample surface from the peak reflectivity. The PhC sample appears to be periodic on average with a varying amount of surface disorder depending on the probing site. The lower reflectivity shown in Fig. 3(a) at wavelengths below the band edge and the initial positive chirp of the input pulses result in a slight steepening of the pulse front and a clipping of the pulse tail  $\sim 180 \text{ fs}$  after the pulse peak. This feature is not as pronounced in the simulations because the band-edge in a perfect PhC is sharp and is therefore only covered by the tail region of a perfect Gaussian pulse spectrum. From Figs. 4(a) and 4(a'), as expected we observe no significant modifications to the pulse envelope.

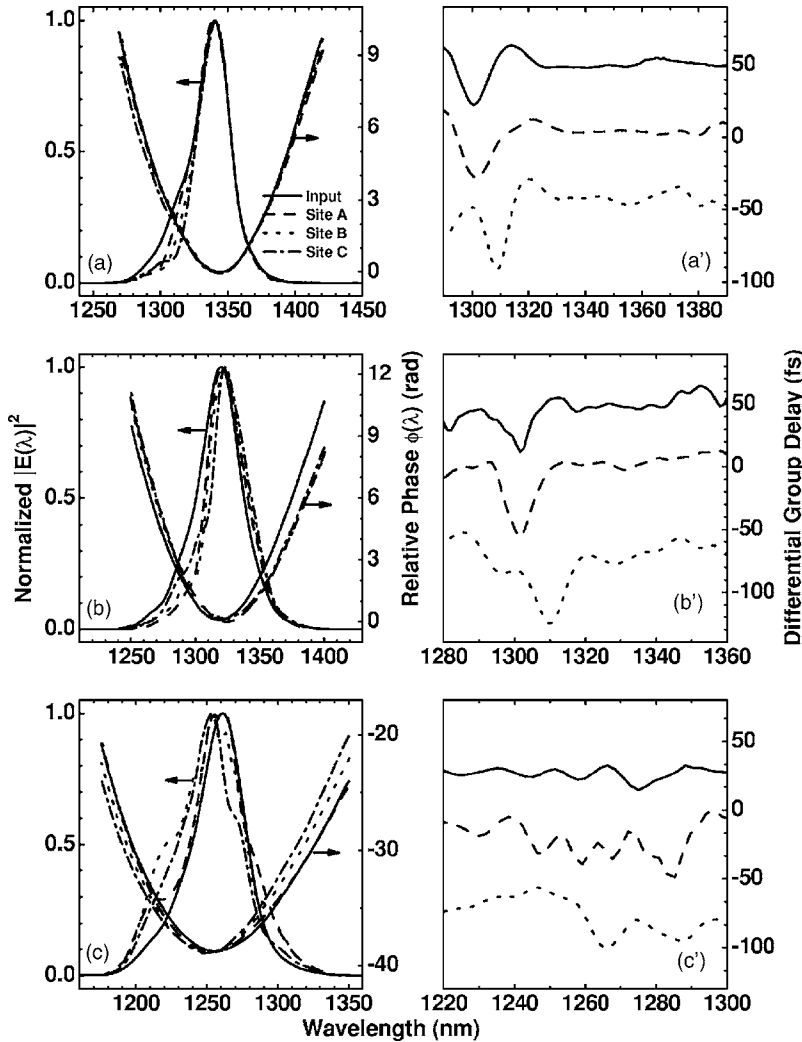


FIG. 4. Spectral intensity and phase of the reflected pulses for  $\lambda_{in}$ ,  $\lambda_{edge}$ , and  $\lambda_{out}$  pulses. Spectra (a) to (c) are the experimentally measured results for  $\lambda_{in}$ ,  $\lambda_{edge}$ , and  $\lambda_{out}$  pulses respectively while (a') to (c') are the differential group delays derived from the phase information shown in (a) to (c), respectively. The differential group delay spectra are displaced vertically for clarity.

lope and phase characteristics for the bandwidth contained within the photonic gap.

(ii) *Pulse centered on band gap edge.* In Fig. 3(b) significant pulse reshaping is seen to occur for the  $\lambda_{edge}$  pulses where the FWHM of the peak appears to be narrowed by 14% to 25%. A distinct shoulder is also visible on the pulse's trailing edge, 200 fs after the peak. The shoulder amplitude depends on the illumination site, varying from 2.5% to 18% of the pulse peak. Similar features also occur in the simulation [Fig. 3(b')] which shows a narrowing of the main peak by 17% as well as a small shoulder ( $\sim 7\%$  of the peak intensity) that develops 250 fs after the main pulse. However, if the input pulse possesses a negative chirp of the same magnitude as the positive chirp, the pulse front rise time increases while the pulse fall time decreases. Consequently, the pulse peak can be delayed by as much as 60% of the input pulse width which itself is broadened by 15%. In either case the reflected pulse profile can be intuitively understood by considering whether the pulse leading edge is dominated by the strongly reflected longer wavelengths or the weakly reflected shorter wavelengths. This is also confirmed by the correlation between the shoulder amplitudes and the spectral shapes of the pulses at shorter wavelengths [evident in Fig. 3(b)]. In the absence of chirp, the simulated pulse peak ap-

pears unperturbed. All the simulation results however show a long but progressively weakening pulse tail; this signature is related to pronounced changes in the dispersive properties of the perfect PhC sample at the band edge. In the time domain, this can be interpreted as multiple coherent scatterings of the pulse within the PhC as it travels with a slow group velocity at the band edge; each scattering event makes a small contribution to the reflected signal. However, this long but weak tail (intensity  $< 1\%$  of the peak) may not always be easily observable due to diffuse scattering by structural defects within the PhC sample. Disorder often leads to the broadening of photonic band structure features<sup>18,19</sup> so that changes in the dispersive properties are not as sharply defined as those from a perfect PhC.

In both Figs. 4(a') and 4(b') the group delay spectra of the  $\lambda_{edge}$  and  $\lambda_{in}$  pulses show a distinct drop of  $\sim 26$  to 54 fs at a wavelength 10 nm below the band edge. The spectral positions of the reduced group delays correspond closely to that of the reflectivity minima shown in Fig. 2. To understand this it should be noted that optical transport in PhC is governed by the interplay between coherent Bragg scattering from a periodic structure and incoherent scattering due to bulk or surface disorder. Even in the presence of disorder, the dispersion curves and surfaces of the PhC still play an im-

portant role and need to be considered carefully.<sup>9,20</sup> Although the incident light is introduced along the  $\Gamma$ - $M$  direction, some light may be scattered by disorder away from the original direction. Consequently, for wavelengths longer than  $\lambda_{\text{edge}}$ , nearby propagating states lying along an  $M$ - $K$  dispersion curve (as shown in Fig. 1) may be excited and the scattered light can thus continue to propagate in the PhC without Bragg attenuation.<sup>8</sup>

However, for  $\lambda > 1330$  nm, most of the light that is not scattered experiences Bragg reflection and the sample reflectivity is relatively high. The group delay in this wavelength regime is thus dependent on the effective penetration depth of the Bragg reflected light. Conversely, some of the scattered light with wavelengths more than 20 nm below  $\lambda_{\text{edge}}$  returns along the specular direction and the group delay in this case is therefore dependent on the photon mean free path due to incoherent scattering within the PhC.<sup>8,21</sup> In the narrow wavelength regime  $\sim 10$  nm below  $\lambda_{\text{edge}}$ , the spectra in Fig. 2 show a dip in the sample reflectivity. From the inset to Fig. 1, it is obvious that in this regime, light at any wavelength can excite two or more eigenmodes simultaneously so it is possible that the coupling between external light and the PhC is improved due to interference between modes.<sup>22</sup> Consequently, most of the specular reflected light is due to surface and near-surface scattering and the group delay is thus shortened. The group delay of Bragg reflected photons does not appear to be too different from the average group delay of the backscattered photons. Although from the band structure one might expect the group delay at the band edge to be very long, this feature is not consistently prominent in the profiles shown in Figs. 4(a') and 4(b'). This is because incoherent scattering makes it difficult to observe the expected slow group velocity in reflection (unlike in transmission) for the short interaction length of the reflected light with the PhC. Scattering can either lead to increased group delay due to the longer dwell time of photons in the sample<sup>23,24</sup> or limit the extent to which group velocity can be slowed down at band edges.<sup>5,25</sup>

It may be worthwhile to consider how one can use the reduced group delay in the transition wavelength regime to characterize the photon mean free paths in the PhC sample. Since the air-fill fraction of the silicon PhC samples is 0.6, the effective refractive index of the sample is therefore  $\sim 2.35$ . In Figs. 4(a') and 4(b'), the minima due to near-surface scattering correspond to an average 45 fs reduction in group delay. The difference between mean free paths of Bragg reflected light and incoherently scattered light in the surface (near-surface) region is therefore  $\sim 6 \mu\text{m}$  (equivalent to eight times the lattice pitch). By comparison, Huang *et al.*<sup>8</sup> estimated a photon mean free path of  $7 \mu\text{m}$  and a Bragg attenuation depth of  $5 \mu\text{m}$  for light backscattered from their opal PhC samples.

(iii) *Pulse centered outside the band gap.* From the band structure shown in Fig. 1, one expects the PhC to introduce quadratic chirp on the  $\lambda_{\text{out}}$  pulse since the central wavelength propagates faster than both the shorter and longer wavelengths. This feature is manifested in the simulated pulse shape as a slight shoulder (with a maximum 60% intensity

increase) 230 fs after the peak, as shown in Fig. 3(c'). However, in the presence of disorder, most of the back-reflected light outside the stopgap is due to dramatic pulse reshaping, related to multiple, incoherent scattering from the PhC. Figure 3(c) shows that the reflected pulses are severely distorted in shape and the pulse widths are broadened by 8% to 48% (FWHM). This is related to the large distribution of path lengths traversed by light so that some escapes from the sample at a shallow depth and some from a larger depth.<sup>24</sup> Any influence of the band structure is thus masked by scattering. As expected, the group delay spectra shown in Fig. 4(c') are noisy with peak-to-peak fluctuations of  $\sim 21$ –46 fs. In comparison, Figs. 4(a') and 4(b') show that the group delay for wavelengths longer than the band edge exhibit weaker peak-to-peak fluctuations of  $\sim 13$ –23 fs. The pulse spectra in Fig. 4(c) are similarly distorted and the bandwidth is increased by 13% to 46%. This increased bandwidth is mainly due to increased scattering at the shorter wavelengths which are more sensitive to sample disorder.<sup>25,26</sup> The specular reflected light has a distorted Gaussian spatial profile with a single centered peak intensity. This is attributed to the finite probability of perpendicular momentum transfer for backscattered photons.<sup>27</sup> The spatial profile however does not have the appearance of a triangular peak superimposed on a diffused background, a signature of enhanced backscattering from 3D PhC and other random media.<sup>8,21,27</sup> This is likely because scattering in the plane of incidence (plane of periodicity) is expected to be different than scattering in the normal direction along the pore axis of the 2D PhC sample.

## V. CONCLUSIONS

In summary, we have shown how the shape of pulses reflected from a photonic crystal is influenced by the interplay between coherent Bragg scattering and incoherent scattering. Bragg reflected pulses experience the periodicity of the PhC sample and their pulse shapes are preserved. Outside the photonic gap, multiple scattering due to bulk or surface disorder leads to distortion in the pulse shape and strong fluctuations in the group delay spectrum. Just below the band edge, the group delay is reduced by  $\sim 45$  fs since most of the reflected light is due to surface and near-surface scattering. From this observation we deduce that the difference in the mean free paths for Bragg scattered photons and incoherently scattered photons in the near-surface region is  $\sim 6 \mu\text{m}$ . At the band edge, the strong asymmetric spectrum produces a shoulder in the trailing edge of the pulse and also causes the peak to appear narrower. Pulses with different chirp characteristics are expected to have different pulse shapes upon reflection near the band edge.

## ACKNOWLEDGMENTS

H.W.T. and H.v.D. gratefully acknowledge the financial support of Photonics Research Ontario and the Natural Sciences and Engineering Research Council of Canada. R.B.W. thanks the DFG in the SPP 113 under Contract No. WE 2637/3.

- <sup>1</sup>J. D. Joannopoulos, R. D. Meade, and J. N. Winn, *Photonic Crystals, Molding the Flow of Light* (Princeton University Press, Princeton, 1995).
- <sup>2</sup>*Photonic Crystals and Light Localization in the 21st Century*, edited by C. M. Soukalis (Kluwer Academic, Dordrecht, 2001).
- <sup>3</sup>L. J. Gamble, W. M. Diffey, S. T. Cole, R. L. Fork, D. K. Jones, T. R. Nelson, Jr., J. P. Loehr, and J. E. Ehret, *Opt. Express* **5**, 267 (1999).
- <sup>4</sup>P. M. Johnson, A. Imhof, B. P. J. Bret, J. G. Rivas, and A. Lagendijk, *Phys. Rev. E* **68**, 016604 (2003).
- <sup>5</sup>A. Imhof, W. L. Vos, R. Sprik, and A. Lagendijk, *Phys. Rev. Lett.* **83**, 2942 (1999).
- <sup>6</sup>T. Tanaka, S. Noda, A. Chutinan, T. Asano, and N. Yamamoto, *Opt. Quantum Electron.* **34**, 37 (2002).
- <sup>7</sup>A. F. Koenderink, A. Lagendijk, and W. L. Vos, *Phys. Rev. B* **72**, 153102 (2005).
- <sup>8</sup>J. Huang, N. Eradat, M. E. Raikh, Z. V. Vardeny, A. A. Zakhidov, and R. H. Baughman, *Phys. Rev. Lett.* **86**, 4815 (2001).
- <sup>9</sup>A. F. Koenderink and W. L. Vos, *Phys. Rev. Lett.* **91**, 213902 (2003).
- <sup>10</sup>V. N. Astratov, A. M. Adawi, S. Fricker, M. S. Skolnick, D. M. Whittaker, and P. N. Pusey, *Phys. Rev. B* **66**, 165215 (2002).
- <sup>11</sup>A. F. Koenderink and W. L. Vos, *J. Opt. Soc. Am. B* **22**, 1075 (2005).
- <sup>12</sup>Since the focused beams converge with a small angle less than  $2.5^\circ$  on the samples, the small fraction of off-normal incidence light is not an issue.
- <sup>13</sup>R. Trebino, *Frequency-Resolved Optical Gating: The Measurement of Ultrashort Laser Pulses* (Kluwer Academic, Boston, 2000).
- <sup>14</sup>The phase-matching acceptance bandwidth for the  $160\ \mu\text{m}$  thick BBO crystal is  $\sim 1\ \mu\text{m}$  at our wavelengths. This is much larger than the  $35\ \text{nm}$  bandwidth of the pulses.
- <sup>15</sup>The FROG errors encountered in all the measurements are very small and lie between 0.0023 and 0.0059 for a grid size of  $256 \times 256$ . These small errors indicate a good agreement between the retrieved and measured FROG spectra.
- <sup>16</sup>SF2 glass has a group velocity dispersion of  $47\ \text{fs}^2/\text{mm}$  at our wavelengths.
- <sup>17</sup>Although the bandwidth of the  $\lambda_{\text{in gap}}$  pulses does not completely lie in the stopgap, the results enabled us to confirm some of the findings for the band edge pulses while still providing insight about how Bragg diffraction in the stopgap may influence the shapes of the reflected pulses.
- <sup>18</sup>J. F. Galisteo Lopez and W. L. Vos, *Phys. Rev. E* **66**, 036616 (2002).
- <sup>19</sup>Y. A. Vlasov, V. N. Astratov, A. V. Baryshev, A. A. Kaplyanskii, O. Z. Karimov, and M. F. Limonov, *Phys. Rev. E* **61**, 5784 (2000).
- <sup>20</sup>M. A. Kaliteevski, J. M. Martinez, D. Cassagne, and J. P. Albert, *Phys. Rev. B* **66**, 113101 (2002).
- <sup>21</sup>A. F. Koenderink, M. Megens, G. van Soest, W. L. Vos, and A. Lagendijk, *Phys. Lett. A* **268**, 104 (2000).
- <sup>22</sup>K. Sakoda, *Optical Properties of Photonic Crystals* (Springer, Heidelberg, 2001).
- <sup>23</sup>Y. A. Vlasov, M. A. Kaliteevski, and V. V. Nikolaev, *Phys. Rev. B* **60**, 1555 (1999).
- <sup>24</sup>J. X. Zhu, D. J. Pine, and D. A. Weitz, *Phys. Rev. A* **44**, 3948 (1991).
- <sup>25</sup>Y. A. Vlasov, S. Petit, G. Klein, B. Honerlage, and C. Hirleimann, *Phys. Rev. E* **60**, 1030 (1999).
- <sup>26</sup>R. Rengarajan, D. Mittleman, C. Rich, and V. Colvin, *Phys. Rev. E* **71**, 016615 (2005).
- <sup>27</sup>A. Lagendijk, R. Vreeker, and P. de Vries, *Phys. Lett. A* **136**, 81 (1989).